1 **Ecological and environmental stability in offshore Southern California**

2 **Marine Basins through the Holocene**

3

4 **Hannah M. Palmer[1,2], Tessa M. Hill[1,2], Esther G. Kennedy[1,2], Peter D. Roopnarine[3], Sonali**

5 **Langlois[4], Katherine R. Reyes[5], and Lowell D. Stott[6]**

6

7    1.  Earth and Planetary Sciences, University of California, Davis

8    2.  Bodega Marine Laboratory, University of California, Davis

9    3.  California Academy of Sciences

10   4.  Santa Rosa Junior College

11   5.  Dominican University of California

12   6.  University of Southern California

13

14 Corresponding author: Hannah M. Palmer (hmpalmer@ucdavis.edu)

15

16 **Key Points:**

17    •  In the Southern California Borderlands, oxygenation below 1400 m was stable and reduced
18       relative to modern from 11.0-4.7 ka

19    •  San Nicolas Basin experienced an oxygenation episode from 4.7-4.3 ka and oxygenation in
20       Tanner Basin increased at 1.7 ka relative to 5.4-1.7 ka

21    •  Variance in reconstructed Holocene dissolved oxygen concentration is similar to decadal scale
22       variance in modern dissolved oxygen

23

24

25

**Abstract**

In the face of ongoing marine deoxygenation, understanding timescales and drivers of past oxygenation change is of critical importance. Marine sediment cores from tiered silled basins provide a natural laboratory to constrain timing and implications of oxygenation changes across multiple depths. Here, we reconstruct oxygenation and environmental change over time using benthic foraminiferal assemblages from sediment cores from three basins across the Southern California Borderlands: Tanner Basin (EW9504-09PC, 1194 m water depth), San Nicolas Basin (EW9504-08PC, 1442 m), and San Clemente Basin (EW9504-05PC ,1818 m). We utilize indicator taxa, community ecology, and an oxygenation transfer function to reconstruct past oxygenation, and we directly compare reconstructed dissolved oxygen to modern measured dissolved oxygen. We generate new, higher resolution carbon and oxygen isotope records from planktic (*Globigerina bulloides*) and benthic foraminifera (*Cibicides mckannai*) from Tanner Basin. Geochemical and assemblage data indicate limited ecological and environmental change through time in each basin across the intervals studied. Early to mid-Holocene (11.0-4.7 ka) oxygenation below 1400 m (San Clemente and San Nicolas) was relatively stable and reduced relative to modern. San Nicolas Basin experienced a multi-centennial oxygenation episode from 4.7-4.3 ka and oxygenation increased in Tanner Basin gradually from 1.7-0.8 ka. Yet across all three depths and time intervals studied, dissolved oxygen is consistently within a range of intermediate hypoxia (0.5-1.5 ml $L^{-1}$ [$O_2$]). Variance in reconstructed dissolved oxygen was similar to decadal variance in modern dissolved oxygen and reduced relative to Holocene-scale changes in shallower basins.

**Plain Language Summary**

Globally, marine oxygenation is declining with detrimental impacts to ecosystems and economies. To better understand the drivers and consequences of ocean oxygen change, we can examine the fossil record to identify how oxygenation changed in the past. Specifically, we use the relative abundance and chemistry of microfossils (i.e., foraminifera) to reconstruct past oxygenation. Here, we examined microfossils from three sediment cores in three basins (Tanner, San Nicolas, San Clemente) off the coast of Southern California. Marine dissolved oxygen (below 1400 m water depth) was relatively stable and lower than modern from 11,000 to 4,700 years before present. San Nicolas Basin experienced a multi-centennial oxygenation episode from 4,700-4,300 years before present and oxygenation increased in Tanner Basin gradually from 2,000-800 years before present. When compared to modern, the range of values of reconstructed oxygen through the entire time studied (thousands of years) is similar to the range of values of modern oxygen at the same depths, indicating that the changes in the last ten thousand years were similar to the amount of change occurring on annual and decadal timescales in the modern ocean.

60 **1  Introduction**

61 **1.1 Marine oxygenation in the past and present**

62 At present, global marine oxygenation is declining due to anthropogenic climate change, with important

63 implications for benthic and pelagic ecosystems (Breitburg et al., 2018; Oschlies et al., 2018; Schmidtko

64 et al., 2017). Ocean oxygenation, particularly at depth, is an important driver of ecosystem zonation, and

65 expansion of oxygen minimum zones (OMZ) is a current threat to global marine ecosystems (Breitburg et

66 al., 2018; Helly & Levin, 2004; Stramma, Schmidtko, et al., 2010). Deoxygenation at depth can be driven

67 by several processes: increased export of organic matter from surface to depth leading to increased

68 respiration below the photic zone, increased stratification (often due to surface warming) reducing

69 ventilation at depth, warming surface temperatures reducing rates of diffusion of atmospheric oxygen into

70 surface waters, and changes in the source, current velocity, or oxygenation of intermediate waters (Levin

71 et al., 2009; Oschlies et al., 2018; Stramma, Schmidtko, et al., 2010).

72

73 Understanding drivers of changes to marine oxygenation in the past is critical for understanding and

74 predicting future change (Jaccard et al., 2014). Paleorecords provide an important archive to investigate

75 temporal and spatial scales of changes to marine oxygenation. In general, warm intervals during the late

76 Quaternary were associated with decreased global ocean oxygenation and cool intervals were associated

77 with increased oxygenation (Cannariato & Kennett, 1999; Cardich et al., 2019; Erdem et al., 2019;

78 Jaccard et al., 2014; Praetorius et al., 2015). The Holocene is an ideal epoch to investigate marine

79 oxygenation because it has well documented intervals of oceanographic change and provides an

80 opportunity to investigate ecological response to stress, including changes to temperature, oxygenation,

81 carbon cycling and ocean circulation (Addison et al., 2017; Barron et al., 2003; Fisler & Hendy, 2008;

82 Moffitt et al., 2015; Praetorius et al., 2015). Over millennial timescales, significant work along the

83 California margin has documented paleoceanographic changes in coastal basins and within the bounds of

84 the modern OMZ (Balestra et al., 2018; Cannariato & Kennett, 1999; Moffitt et al., 2014; Taylor et al.,

85 2015). However, additional work is needed to constrain the timing and extent of oxygenation change

86 below 1000 m, the relative impacts of surface processes and source waters on seafloor oxygenation, and

87 how oxygenation at these depths responds to global and regional environmental change.

88

89 **1.2 Southern California modern and paleoceanography**

90 In the modern California Current eastern boundary upwelling system, an OMZ exists at approximately

91 500 – 1000 m water depth and is an important driver of ecosystem zonation, impacting species

92 distributions in pelagic and seafloor communities (Helly & Levin, 2004; Stramma, Johnson, et al., 2010).

93 The combination of high productivity, high export of organic matter, and age of water masses entering the

94    North Pacific at depth make this a particularly thick and laterally extensive OMZ (Bograd et al., 2008,

95    2019; Evans et al., 2020). The California Margin OMZ is expanding in intensity (decreasing dissolved

96    oxygen), horizontal extent, and vertical thickness (shoaling) (Schmidtko et al., 2017; Stramma, Johnson,

97    et al., 2010). Changes to the OMZ are caused by reductions in the oxygenation of source water and

98    reduced ventilation due to surface warming and stratification (Bograd et al., 2008; Evans et al., 2020). Off

99    the coast of California, dissolved oxygen decreased at a rate of up to 0.047 ml/L/year from 1984-2006 in

100   the upper 500 m of the water column (Bograd et al., 2008, 2015). In the Southern California Current

101   System, 81% of observed change in oxygenation in the upper 400 m of the water column from 1993-2018

102   can be attributed to changes in oxygenation of source waters (Evans et al., 2020).

103

104   In the modern system, Southern California Borderlands surface water flow is counterclockwise (Southern

105   California Eddy), with the western margin dominated by the southward flowing California Current and

106   the eastern margin driven by the northward-flowing California Countercurrent and Davidson Current. At

107   depth, the California Undercurrent flows south to north and is comprised of a mix of Southern

108   Component Intermediate Water from the eastern tropical Pacific and northerly sourced North Pacific

109   Intermediate Water (Balestra et al., 2018; Bograd et al., 2019; Checkley & Barth, 2009; Stott et al., 2000;

110   Talley, 1993). Offshore Southern California, a series of submarine basins, generally deepening from north

111   to south, structure intermediate and deep-water flow (Berelson, 1991; Berelson & Stott, 2003).

112   Oxygenation in basinal environments is impacted by the export of organic matter from overlying surface

113   waters, advection of intermediate and deep waters that spill into the basin, and within basin processes,

114   including sediment and pelagic biogeochemical cycles. By examining the environments of multiple silled

115   basins, the effects of water advection can be separated from surface processes and the depths of

116   significant biogeochemical change can be determined.

117

118   The California margin OMZ fluctuated throughout the Holocene (Balestra et al., 2018; Christensen et al.,

119   1994; McGann, 2011; Moffitt et al., 2014; Palmer et al., 2020). Previous analyses of marine sediment

120   cores from the Santa Barbara Basin (SBB) document intervals of hypoxia in the early Holocene (11.5-10

121   ka) followed by oscillations in the strength of the OMZ from 10-6 ka with several intervals of hypoxia

122   (less than 0.5 ml $L^{-1}$ [$O_2$]) and an increase in oxygenation in the last 6 ka within SBB, yet the OMZ

123   persists throughout the Holocene (Moffitt et al., 2014; Ohkushi et al., 2013; Wang et al., 2020). In Santa

124   Monica Basin (SMB), severe hypoxia (less than 0.3 ml $L^{-1}$ [$O_2$]) was present from the start of the

125   Holocene to 9 ka, and the mid to late Holocene (9-0 ka) had weaker hypoxia (0.3-1.5 ml $L^{-1}$ [$O_2$]) than the

126   early Holocene (Balestra et al., 2018). The modern OMZ, with oxygen levels at 0-1.5 ml $L^{-1}$ [$O_2$],

127   developed in the mid to late Holocene (by 6-4 ka) across the broader North Pacific (Addison et al., 2017;

128    McGann, 2011; Ohkushi et al., 2013; Praetorius et al., 2015). Over the past several centuries the SMB

129    experienced variable degrees of dysoxia at interannual to interdecadal time scales (Christensen et al.,

130    1994). These changes are attributable to variable biological carbon flux and respiration at depth (Berelson

131    and Stott, 2003; Stott et al, 2000), underscoring how sensitive the shallow-silled basins are to small

132    changes in biological productivity. Previous analysis of ecosystem responses (benthic foraminiferal and

133    invertebrate) to oxygenation change through the Holocene from the SBB indicate that intervals within the

134    Holocene exhibit distinct phases of ecosystems that do not repeat or overlap, as the oxygen minimum

135    zone and carbon maximum zone fluctuate (Moffitt et al., 2015; Myhre et al., 2017).

136

137    Here, we utilize records from three offshore basins to constrain changes in ocean oxygenation through the

138    Holocene and resultant impacts on benthic ecosystems. Silled basins provide a unique opportunity to

139    examine both local changes within each basin and to compare oxygenation history across depths when

140    records overlap temporally. Combining a series of silled basins allows for the examination of change

141    through time at multiple water depths and sill depths to investigate the relative impact of surface

142    processes and intermediate water changes in determining oxygenation at depth (Balestra et al., 2018;

143    Moffitt et al., 2014; Wang et al., 2020).

144

145    **1.3 Benthic foraminiferal assemblages as a metric of past oxygenation and organic matter export**

146

147    Benthic foraminiferal assemblages are an effective and established metric to quantify past changes in

148    marine oxygenation (Balestra et al., 2018; Belanger et al., 2020; Bernhard et al., 1997, 2003; Bernhard &

149    Gupta, 1999; Cardich et al., 2015, 2019; Caulle et al., 2014; De & Gupta, 2010; Kaiho, 1994; Moffitt et

150    al., 2014; Murgese & De Deckker, 2005; Ohkushi et al., 2013; Praetorius et al., 2015). Benthic

151    foraminiferal assemblages are sensitive to small changes in oxygenation in the North Pacific, even in

152    suboxic environments, not exclusively across large biological thresholds of anoxic or sulfidic conditions

153    (Sharon et al., 2021). Multiple methodologies are used to interpret past environmental change from

154    benthic foraminiferal assemblages, which we introduce and review below.

155

156    Quantifying absolute and relative abundance of benthic foraminiferal species is an established and

157    foundational method; typically, studies quantify species downcore and interpret trends through time using

158    observational or statistical approaches (e.g. Moffitt et al., 2014; McGann, 2011; Gardner et al., 1988).

159    Studies of modern benthic foraminifera from multiple depositional environments and oxygenation

160    regimes have identified oxygenation affinity of benthic foraminiferal species that can be used as indicator

161    species of change through time; this method is most useful to reconstruct relative oxygenation or to

162 identify past oxygenation thresholds (e.g. Cannariato and Kennett, 1999; Palmer et al., 2020; Balestra et

163 al., 2018; Bernhard and Gupta, 1999).

164

165 While these approaches provide relative oxygenation history, transfer functions are used to translate

166 whole or partial benthic species assemblages into absolute oxygenation values (Behl & Kennett, 1996;

167 Kaiho, 1994, 1999; McGann, 2011; Moffitt et al., 2014; Ohkushi et al., 2013; Sharon et al., 2021). Multi-

168 species transfer functions including the Kaiho Benthic Foraminiferal Oxygenation Index, Schmiedl

169 Dissolved Oxygen Index, and Behl Dissolved Oxygen Index are used to generate absolute values of past

170 oxygenation by transforming the relative abundance of species into ml $L^{-1}$ [$O_2$] (Kaiho, 1994; Ohkushi et

171 al., 2013; Sharon et al., 2021). Transfer functions have typically been constructed using case studies from

172 very low oxygen environments (such as Santa Barbara Basin) or by using the lowest known oxygen

173 tolerance for a species; as such, this approach generates inherently conservative (lower) predictions of

174 oxygenation, with the exception of the analysis by Sharon et al., 2021 which utilized multivariate

175 statistical analysis to group species by oxygenation (Kaiho, 1994; Ohkushi et al., 2013; Sharon et al.,

176 2021). Categorization of species into oxic, intermediate hypoxic, and anoxic environments used in

177 multiple transfer functions and as indicator species varies by author (Bernhard et al., 1997; Bernhard &

178 Gupta, 1999; Cannariato & Kennett, 1999; Kaiho, 1994; Moffitt et al., 2014; Palmer et al., 2020;

179 Praetorius et al., 2015). Here we follow the convention: weakly suboxic/oxic ([$O_2$] >1.5 ml $L^{-1}$),

180 intermediate hypoxic/suboxic ([$O_2$] 1.5-0.5 ml $L^{-1}$), and severe hypoxic/dysoxic ([$O_2$] <0.5 ml $L^{-1}$)

181 (Moffitt et al., 2014; Palmer et al., 2020; Sharon et al., 2021; Tetard et al., 2021).

182

183 Recent work on paleoecological assemblages, including benthic foraminifera, utilizing analysis of

184 diversity, richness, and multidimensional statistical analysis has expanded our breadth of understanding

185 of how oxygenation impacts seafloor ecosystems (Belanger et al., 2020; Myhre et al., 2017; Sharon et al.,

186 2021). Ecological analysis provides community-scale assessments of environmental change over time and

187 often complements analysis of indicator taxa or transfer function calculations (Belanger et al., 2020;

188 Myhre et al., 2017; Sharon et al., 2021). In addition to taxonomic evaluation of benthic foraminifera,

189 studies are increasingly relying on morphometrics to assess past environments. These studies are

190 predicated on morphological response or adaptation to oxygenation such as pore density, size, and shape

191 (i.e., roundedness) and are used in both taxon-specific and taxon-independent analyses (Keating-Bitonti &

192 Payne, 2016, 2018; Keating-Bitonti & Payne, 2017; Rathburn et al., 2018; Tetard et al., 2021). Typically,

193 smaller, thin-walled, elongate species are indicative of low oxygen environments in which high-surface

194 area to volume ratio is advantageous, to maximize oxygen absorption, while in well oxygenated

195    environments, larger, thick-walled and porcelaneous taxa with rounded shapes are dominant (Tetard et al.,
196    2021).
197
198    Importantly though, oxygenation is not the only driver of benthic foraminiferal assemblages. Food
199    availability, driven by the timing (pulsed vs. constant) and amount of export of organic matter, water
200    depth, sediment grain size, and water temperature play an important role in structuring seafloor
201    ecosystems, including benthic foraminiferal assemblages (Belanger et al., 2012, 2020; Kaiho, 1999;
202    Venturelli et al., 2018). Here we employ stable isotope and benthic foraminiferal assemblage analyses to
203    investigate cores from three silled basins in the Southern California Borderlands. By combining multiple
204    approaches to assemblage analysis as listed above, we quantify changes in oxygenation below 1000 m,
205    deconstruct surface vs. advective processes as drivers of change, and investigate changes in source
206    waters. This multi-site, multi-faceted approach allows us to reconstruct change over time in each basin
207    and to assess regional scale oxygenation history and environmental change in the Southern California
208    Borderlands through the Holocene.
209
210    **2 Methods**
211    **2.1 Study site**
212    Cores were collected from three silled basins within the Southern California Borderlands (Figure 1).
213    Tanner Basin is located west of the Channel Islands and is the farthest offshore. The basin has a sill depth
214    of 1160 m and a bottom depth of approximately 1500 m (Figure 1). San Nicolas Basin is located south of
215    San Nicolas Island and west of San Clemente Island. The basin has a sill depth of 1100 m and a bottom
216    depth of approximately 1800 m (Figure 1). San Clemente Basin is located south of San Clemente Island
217    and is the deepest site explored here. The basin has a sill depth of 1815 m and a bottom depth of
218    approximately 1950 m (Figure 1). The water depth of each core was assessed at time of core collection
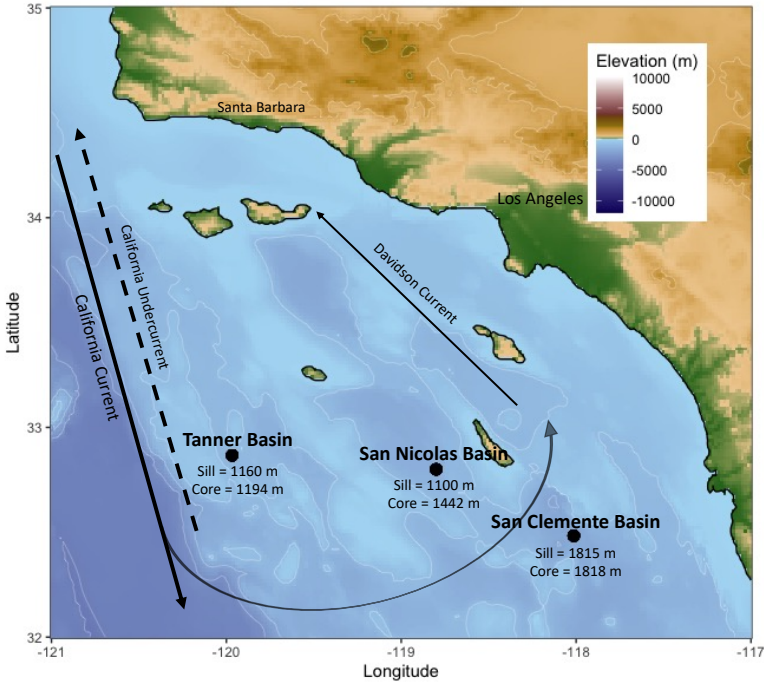219    and bottom depths of each basin were measured using GeoMapApp.

220

**Figure 1:** Map of the locations of the three cores used in this study. Schematic of current locations and directions included, solid lines indicate surface currents (California Current and Davidson Current), dashed line indicates subsurface current (California Undercurrent). The sill depth and core collection depth for each core is reported in meters.

**2.2 Sediment cores**

We investigate three piston cores collected from the Southern California Borderlands on the Maurice Ewing Cruise 9504 in May - June 1995: EW 9504-09PC from Tanner Basin at 1194 m water depth, EW 9504-08PC from San Nicolas Basin at 1442 m water depth, and EW 9504-05 from San Clemente Basin at 1818 m water depth. All cores have 10.16 cm inner diameter and were split and sampled at 2 cm intervals aboard the ship (initial volume of all samples was 162.15 cm$^3$). Sediments from the working half of the core were disaggregated in sodium hexametaphosphate washed over a 63 µm sieve (see Stott et al. 2000). Sediments were dried and stored in glass vials at the University of Southern California until they were processed for this study. The core from Tanner Basin (EW 9504-09PC) was examined from 0-40 cm at 2 cm intervals; intervals below 40 cm were not available for analysis (total of 19 intervals examined). The core from San Nicolas Basin (EW 9504-08PC) was examined at 2 cm intervals from 0-22 cm and every 6 cm from 24-64 cm (due to sample availability, total of 19 intervals examined).  The core from San Clemente Basin (EW 9504-05) was examined at 2 cm intervals from 30-52 cm; intervals from 0-30 cm in EW9504-05 did not have sufficient foraminifera for robust analysis (see below) and were thus excluded from analysis (total of 11 intervals examined). Analysis was conducted at the resolution available to the

241    authors and all intervals with sufficient sediment volume and foraminifera (see below) were used in the

242    study.

243

**2.3 Radiocarbon dating and age model development**

245    Radiocarbon based age models were developed for each core using a combination of previously published

246    and newly generated planktic radiocarbon ages (Table S1, Figure S1). Five age dates within the Holocene

247    (1 San Clemente, 1 Tanner, 2 San Nicolas) were previously measured (Stott et al., 2000). These AMS $^{14}$C

248    ages were completed using bulk planktonic foraminifera (weight ~3-5 mg) analyzed at the Lawrence

249    Livermore National Laboratory (Stott et al., 2000). Three additional radiocarbon dates (1 San Clemente, 2

250    Tanner, 1 San Nicolas) from bulk planktic foraminifera were analyzed in this study. All samples for

251    radiocarbon analysis were prepared by picking shell material from the >150 µm fraction, rinsing shells in

252    methanol, sonicating in methanol for 5-10 seconds, and rinsing twice with deionized water. Shells were

253    then dried in a 60$^O$C drying oven. Radiocarbon analysis was completed at the Lawrence Livermore

254    National Laboratory using $\delta^{13}$C assumed values following the convention of Stuiver and Polach (1977).

255    The reported age is given in radiocarbon years using the Libby half-life of 5568 years. Accelerator mass

256    spectrometry ages were converted to calendar ages before present (BP) by calibration against the

257    Marine20 curve using the open-source software "R" package Bchron (Haslett & Parnell, 2008; Heaton et

258    al., 2020). Calibration included correction for reservoir ages for the Southern California Coast of 220.0 ±

259    40.0 years (Ingram & Southon, 1996; Stuiver & Polach, 1977). Age/depth models for each core were

260    generated using the Bayesian age-depth modeling functionality of Bchron (Table S1, Figure S1).

261

**2.4 Stable Isotope Analysis**

263    Stable isotope analyses from planktic and benthic foraminifera from EW9504-09 (Tanner Basin) were

264    conducted on *Globigerina bulloides* planktic foraminifera and *Cibicides mckannai* benthic foraminifera

265    from 0-40 cm at 2 cm intervals. Samples were prepared by picking from the >150 µm size fraction (2-5

266    individual *C. mckannai* per interval, 15-25 *G. bulloides* per interval) and cleaned using the same

267    methodology as above. Planktic foraminifera were analyzed at the UC Davis Stable Isotope Laboratory

268    and benthic foraminifera were analyzed at the UC Santa Cruz Stable Isotope Laboratory.

269

270    Planktic carbon and oxygen isotope samples were analyzed using a GasBench II system interfaced with a

271    Delta V Plus Isotope Ratio Mass Spectrometer at the UC Davis Stable Isotope Laboratory using standard

272    UCD-SM92 (-1.94 for $\delta^{18}$O and 2.08‰ $\delta^{13}$C) (Ostermann 2000). Values for $\delta^{13}$C and $\delta^{18}$O are expressed

273    in per mil (‰) relative to Vienna Pee Dee Belemnite, and values are corrected for changes in linearity and

274    instrumental drift. Benthic carbon and oxygen isotope samples were analyzed at the UC Santa Cruz Stable

275  Isotope Laboratory by acid digestion using an individual vial acid drop Themo Scientific Kiel IV

276  carbonate device interfaced to Thermo Scientific MAT 253 dual-inlet isotope ratio mass spectrometer. All

277  samples were measured with several replicates of the externally calibrated Carrera Marble in-house

278  standard reference material 'CM12' and the NBS-18 limestone international standard reference material.

279  Values for $\delta^{13}C$ and $\delta^{18}O$ are expressed in per mil (‰) relative to Vienna Pee Dee Belemnite, and values

280  are corrected for changes in linearity and instrumental drift. Data were combined with previously

281  published records of planktic oxygen isotopes and benthic oxygen and carbon isotopes from the same

282  core examined here (EW9504-09) to increase replicates in the late Holocene and to extend the record

283  through the entire Holocene (Stott et al., 2000). As such, isotope records reflect analyses from three

284  different laboratories. Instrument precision from all labs for $\delta^{13}C$ calcite was 0.05-0.06‰ and for $\delta^{18}O$

285  calcite was 0.06-0.10‰. Thus, we report the maximum uncertainty of 0.06‰ for $\delta^{13}C$ calcite and 0.10‰

286  for $\delta^{18}O$ calcite (Figure 3).

287

288  **2.5 Benthic Foraminiferal Assemblages**

289  Samples were dry sieved over a 150 µm sieve and picked for benthic foraminifera. Foraminifera greater

290  than 150 µm have been documented to capture the range of environmental variability in

291  paleoceanographic reconstructions as well as assemblages containing smaller foraminifera and the use of

292  larger specimens results in reduced error in identification (Cannariato & Kennett, 1999; Caulle et al.,

293  2014; Fenton et al., 2018; Palmer et al., 2020). Foraminifera in the size fraction below 150 µm were

294  excluded from this analysis which may have excluded some smaller taxa or smaller individuals of the taxa

295  identified here. Individual foraminifera were picked and identified from each interval to obtain >90

296  individuals per sample (Kemp et al., 2020), as sample sizes as low as 58 have been shown to have stable

297  assemblages (Belanger et al., 2020; Forcino et al., 2015). The average number of individual foraminifera

298  identified in each interval was 230, with a range of 90-665. Samples were mounted on micropaleontology

299  slides using gum tragacanth at time of identification and are archived in the Ocean Climate Laboratory at

300  the UC Davis Bodega Marine Laboratory. Cores were not laminated; thus, bioturbation is expected and

301  may have had an averaging effect on assemblages.

302

303  **2.6 Foraminiferal morphometrics**

304  Morphometrics of benthic foraminifera, including length, width, and surface area were measured using

305  ImageJ software. Length and width of each individual was measured to the longest and widest margins of

306  the shell. Three species were selected for analysis to represent a gradient of oxygenation affinity:

307  *Quinqueloculina* sp. is weakly suboxic/oxic and *B. spissa* and *U. peregrina* are categorized as suboxic

308  (Table S2). Measurements of *Quinqueloculina* sp. and *B. spissa* were quantified in Tanner Basin at 2 cm

309     intervals from 0-40 cm, measurements of *Quinqueloculina* sp. and *U. peregrina* were quantified in San

310     Clemente Basin at 2 cm intervals from 30-44 cm. From each interval, 3-30 individual shells of each

311     species were measured (based on availability of taxa). Results of morphometric analysis were compared

312     to morphometric data (collected using the same methodology) from five open coastal margin sites (300-

313     1175m) near San Diego (see Palmer et al., 2020 for further explanation of the open margin study site, all

314     morphometric data is available on Dryad, see Palmer et al., 2022).

315

316     **2.7 Metazoan microfossil assemblages**

317     In addition to picking and identifying benthic foraminifera, ostracods (Arthropoda - Ostracoda) and

318     urchin spines (Echinodermata) were picked from the 150 μm sediment fraction at all intervals examined.

319     Samples were mounted on micropaleontology slides using gum tragacanth at time of identification and

320     are archived in the Ocean Climate Laboratory at the UC Davis Bodega Marine Laboratory. Due to low

321     abundances, presence/absence is recorded, rather than relative abundance.

322

323     **2.8 Benthic foraminiferal oxygenation index**

324     Oxygenation was reconstructed using two modified benthic foraminiferal oxygenation indices: Behl and

325     Schmiedl (Schmiedl et al., 2003; Sharon et al., 2021). Data were analyzed using both indices in order to

326     compare the results; the Schmiedl Index uses diversity as a input, but does not include suboxic taxa, while

327     the Behl Index does not include diversity, but includes oxic, suboxic, and weakly suboxic/dysoxic taxa

328     (Ohkushi et al., 2013; Schmiedl et al., 2004). Using a combination of paleo and modern samples, Sharon

329     et al., 2021 used detrended correspondence analysis (DCA) to expand the list of species that can be used

330     as inputs to the Behl Index, thus allowing for its application in a broader range of seafloor environments

331     (Sharon et al., 2021). Here we utilize the Behl dissolved oxygen index following Ohkushi et al., 2013, but

332     expand the list of species included in the assessment following the work of Sharon et al., 2021. We

333     further modified the list of species used in the Behl and Schmiedl indices by adding ten additional species

334     using previously published oxygenation affiliations and morphometric or taxonomic similarities (Table

335     S2). We included all species that made up at least 2% of the total foraminifera identified across all time

336     intervals and cores examined. Oxygenation reconstructions were calculated using two equations:

337     Behl DO index = ((dysoxic % * 0.1) + (suboxic % * 0.5) + (weakly suboxic/oxic % * 1.5) )/100 and

338     Schmiedl index = ((weakly suboxic/oxic %)/(weakly suboxic/oxic % + hypoxic %) + diversity (H`)) * 0.5

339     (Ohkushi et al., 2013).

340

341     **2.9 Statistical analysis**

342      Diversity of each interval was calculated using Shannon Index (H). Richness was calculated by tabulating

343      the number of distinct species present in an interval. Non-metric multidimensional scaling (NMDS)

344      ordination, using square root transformation of assemblage species counts and Bray-Curtis similarities

345      and detrended correspondence analysis were conducted and compared (Figure S2, Table S3, S4). We used

346      a single factor ANOVA to determine if there were significant differences among mean morphometrics

347      (length, width, surface area), diversity between basins, diversity through time, and values of reconstructed

348      vs. modern oxygenation. If the results of ANOVA were significant, we performed Tukey's Test to

349      determine where differences in the means occurred. All statistical analyses were completed using the

350      Vegan R package (nmds function, decorana function)  or base R functions (tukeyHSD function and

351      res.aov function) (Oksanen et al., 2013; R Core Team, 2021).

352

353      **2.10 Modern oxygenation data**

354      Modern oxygen data were sourced from the California Cooperative Oceanic Fisheries Investigations

355      (CalCOFI) for the years 1949-2019. Data were included from all sites in the CalCOFI sampling grid

356      bounded by -116° – -121° W longitude and 32° – 34.5° N latitude (Point Conception is northern

357      boundary)) and depths 1000-2000 m to maximize data availability. Oxygenation was calculated using

358      Winkler Titration of bottle samples at the Scripps Institution of Oceanography (Bograd et al., 2003;

359      Bograd & Lynn, 2003). Flagged data from CalCOFI and property-property and time series analysis

360      excluded 19 data points. The CalCOFI data set used here includes a total of 272 modern oxygen

361      measurements.

362

363      **3     Results**

364      **3.1 Age Model Development**

365      Age models produced a median age and probability distribution (at a range of 95.0% uncertainty, 2σ) at

366      each depth (Figure S1). Age model uncertainty is reported in Table S2.  Coherence of age model within

367      each core and between cores supports use of this age model (Figure S1). Mean sedimentation rates for the

368      entire Holocene are similar for all three cores: Tanner has a mean sedimentation rate of 10.8 (± 1σ =5.3

369      cm/ka), San Nicolas has a mean sedimentation rate of 9.9 (± 1σ =1.8 cm/ka), and San Clemente has a

370      mean sedimentation rate of 12.0 (± 1σ =4.8 cm/ka). Sedimentation rates reported here are similar to those

371      observed offshore Central California through the Holocene (McGann, 2011). All following results are

372      discussed as age in thousands of years before present (ka).

373

374      **3.2 Benthic foraminiferal assemblages**

375   Benthic foraminiferal assemblages were quantified down core for each core in which sufficient benthic

376   foraminifera were present (Tanner Basin 0-40 cm at 2 cm intervals, San Nicolas Basin 0-22 cm at 2 cm

377   intervals, 24-66 at 6 cm intervals, San Clemente Basin 30-54 cm at 2 cm intervals). The total number of

378   species (richness) in each sample ranged from 15 to 24 (Figure S4) and species diversity (Shannon Index,

379   H) ranged from 2.12 to 2.68, with a mean of 2.40 ($\pm$ 1$\sigma$ = 0.15) across all three basins (Figure S4).

380   Species diversity (H) is significantly higher in Tanner Basin (mean=2.51, $\pm$ 1$\sigma$ = 0.11), relative to San

381   Nicolas Basin (mean=2.30, $\pm$ 1$\sigma$ = 0.11) and San Clemente Basin (mean=2.37, $\pm$ 1$\sigma$ = 0.10) (ANOVA,

382   Tukey Test p<0.05) (Figure 3).  Comparison of diversity through time in individual basins using 0.5 or 1

383   ka time bins shows that diversity (H) is not statistically different through time in Tanner, San Nicolas, and

384   San Clemente basins (ANOVA, Tukey Test p<0.05 for all sites). Multivariate statistical analysis using

385   nonmetric multidimensional scaling (NMDS) and detrended correspondence analysis (DCA) of down-

386   core assemblages shows that, through time, assemblage similarity within sites exceeds similarity to

387   assemblages at any other site (Figure S2). Comparison of results of DCA and NMDS with previously

388   published benthic foraminiferal species categorization by oxygenation do not clearly indicate that

389   oxygenation is the dominant factor in controlling species assemblage at the community level.

390

391   In Tanner Basin, the most common species (in descending order) are *B. spissa, G. subglobosa, H.*

392   *soldanii, Quinqueloculina* sp., and *P. murrhina* (Figure 2). Species diversity (H) ranged from 2.32-2.68

393   with a mean of 2.51 ($\pm$ 1$\sigma$ = 0.11) (Figure 3). Benthic foraminiferal assemblage gradually changed from

394   5.5 – 1.9 ka; this shift is largely driven by a gradual increase in *Hansenisca soldanii* (previously

395   *Gyroidina soldanii*) and decrease in *B. spissa* and *U. peregrina* (Figure 2). *G. subglobosa* and

396   *Quinqueloculina* sp consistently make up 10-20% of the assemblage through time (Figure 2).  In San

397   Nicolas Basin, the most common species (in descending order) are *U. peregrina, E. pacifica, C.*

398   *mckannai, B. spissa,* and *Uvigerina* sp (Figure 2). Species diversity (H) ranges from 2.12-2.56 with a

399   mean of 2.30 ($\pm$ 0.11) (Figure 3). The assemblage in San Nicolas Basin exhibits little change through time

400   from 10.1-4.7 ka when *U. peregrina* makes up 15-45% of the assemblage. From 4.7-4.2 ka, there is a

401   sharp decline in *U. peregrina* and a sharp increase in *C. mckannai* (Figure 2). From 4.0-1.9 ka, the trend

402   reverses, and the assemblage is very similar to the assemblage from 10.1-4.7 ka. In San Clemente Basin,

403   the most common species (in descending order) are *U. peregrina, C. mckannai, E. pacifica,*

404   *Quinqueloculina* sp., and *Uvigerina* sp (Figure 2). Species diversity (H) ranges from 2.17-2.51 with a

405   mean of 2.37 ($\pm$ 0.10) (Figure 3). In San Clemente Basin, relative abundance of benthic foraminifera

406   exhibits little change over time from 11.2-7.1 ka as shown by both individual species analysis and DCA
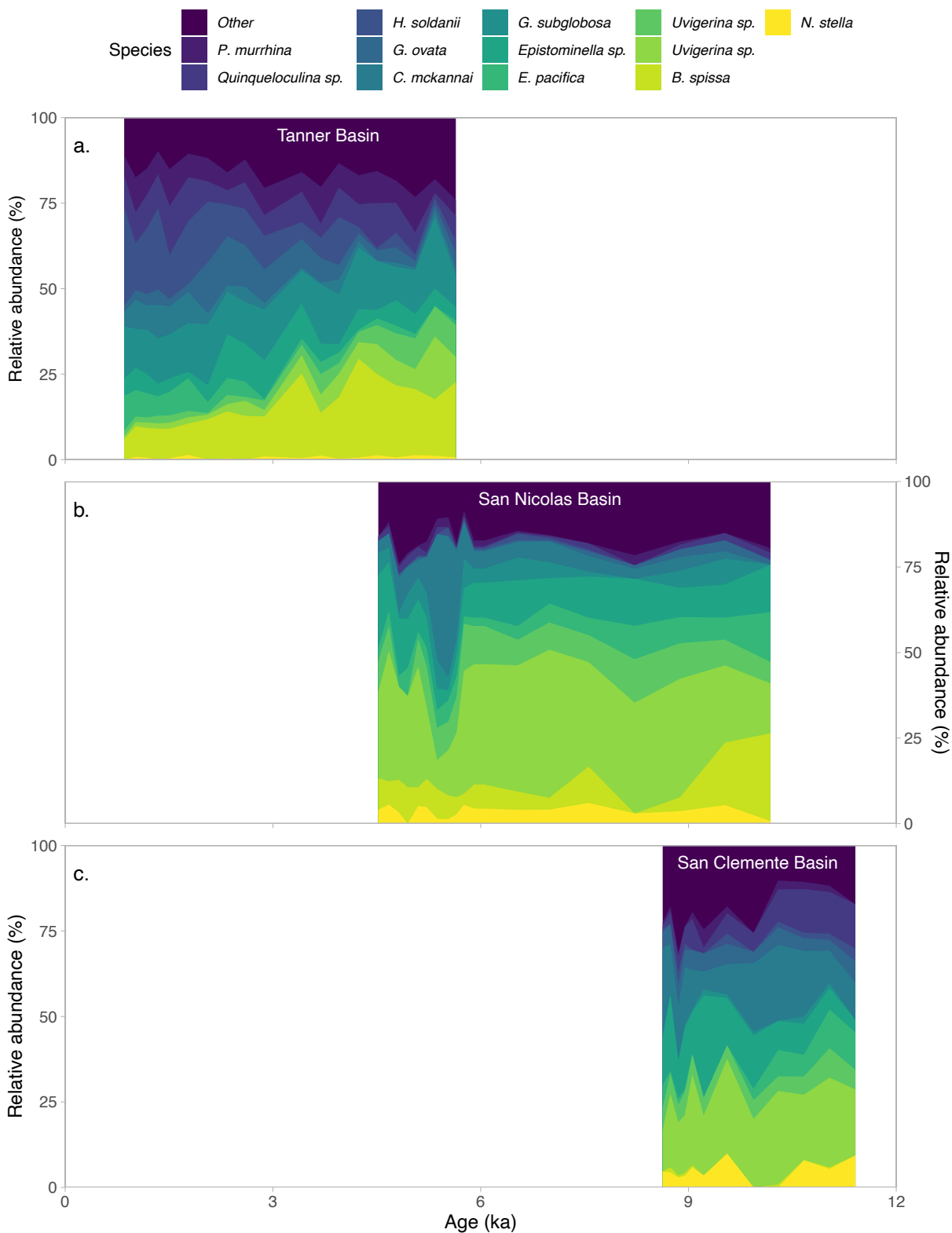
407   (Figure S2).

408

409 **Figure 2:** Relative abundance of benthic foraminifera vs. age in thousands of years before present for

410 three cores examined here: Tanner (a.), San Nicolas (b.), and San Clemente (c.). Ten most abundant

411     species are shown; all other species grouped as "other." Each color represents a taxonomic group

412     (species, genus, or other). See legend at top of plot for color of each. Taxa colors are ordered from

413     dysoxic indicator taxa (yellow/bottom of plot) to oxic indicator taxa (blue/top of plot).

414

### 3.3 Shell morphometrics

415

416     Shell size was quantified to examine sub-lethal impacts of environmental change on benthic fauna. Shell

417     size, measured as length, width, and surface area of three taxa (*U. peregrina, Quinqueloculina* sp., and *B.*

418     *spissa*) was compared across the three cores examined here and to size data from a suite of cores from the

419     San Diego Margin (Palmer et al., 2020). Shell size of *U. peregrina* is statistically significantly larger in

420     coastal sites (p<0.05) relative to San Clemente basin (Figure S3a). Shell size of *B. spissa* is statistically

421     significantly larger in coastal sites (p<0.05) relative to Tanner Basin (Figure S3a). Shell size of *B. spissa*

422     and *Quinqueloculina* from Tanner Basin show relatively little variability through time (5.5-1.9 ka)

423     (Figure S3b, c). As all metrics of shell size (length, width, and surface area) show the same trends, further

424     discussion uses only shell surface area as a metric of whole shell size.

425

### 3.4 Reconstructed oxygenation using transfer functions

426

427     Reconstructed dissolved oxygen using the Behl Index ranges from 0.56-1.12 ml L$^{-1}$ with a mean of 0.79

428     ml L$^{-1}$ (Figure S4) and varies across basins: Tanner Basin mean is 0.86 ml L$^{-1}$ and ranges from 0.59-1.12

429     ml L$^{-1}$, San Nicolas Basin mean is 0.67 ml L$^{-1}$ and ranges from 0.56-1.02 ml L$^{-1}$, and San Clemente Basin

430     mean is 0.84 ml L$^{-1}$ and ranges from 0.68-0.96 ml L$^{-1}$. Reconstructed dissolved oxygen using the

431     Schmiedl Index ranges from 1.36-1.81 ml L$^{-1}$ for all three cores, with a mean of 1.62 ml L$^{-1}$ (Figure S4).

432     Schmiedl Index reconstructed oxygenation varies across basins: Tanner Basin mean is 1.73 ml L$^{-1}$ and

433     ranges from 1.59-1.81 ml L$^{-1}$, San Nicolas Basin mean is 1.50 ml L$^{-1}$ and ranges from 1.36-1.66 ml L$^{-1}$,

434     and San Clemente Basin mean is 1.60 ml L$^{-1}$ and ranges from 1.48-1.71 ml L$^{-1}$.  Importantly, the number

435     of individual foraminifera identified did not impact the outcomes of the Behl or Schmiedl indices (Figure

436     S4). Species richness is not correlated with outputs of the Behl Index, but is positively correlated with the

437     Schmiedl Index (Figure S4).

438

### 3.5 Stable isotope record

439

440     Stable isotope records from Tanner Basin varied slightly through time (Figure 3). Analysis of planktic

441     oxygen and carbon isotopes from *G. bulloides* yielded the following: $\delta^{13}$C mean is -0.59 (± 1$\sigma$ = 0.25),

442     range is -0.92 to -0.05, $\delta^{18}$O mean is 0.22 (± 1$\sigma$ = 0.31), range is -0.15 to 1.08 (Figure 3). Analysis of

443     benthic oxygen and carbon isotopes from *C. mckannai* yielded the following: $\delta^{13}$C mean is -0.03 (± 1$\sigma$

444     =0.07), range is -0.13 to 0.10, $\delta^{18}$O mean is 2.53 (± 1$\sigma$ = 0.17), range is 2.29 to 2.73 (Figure 3).

445
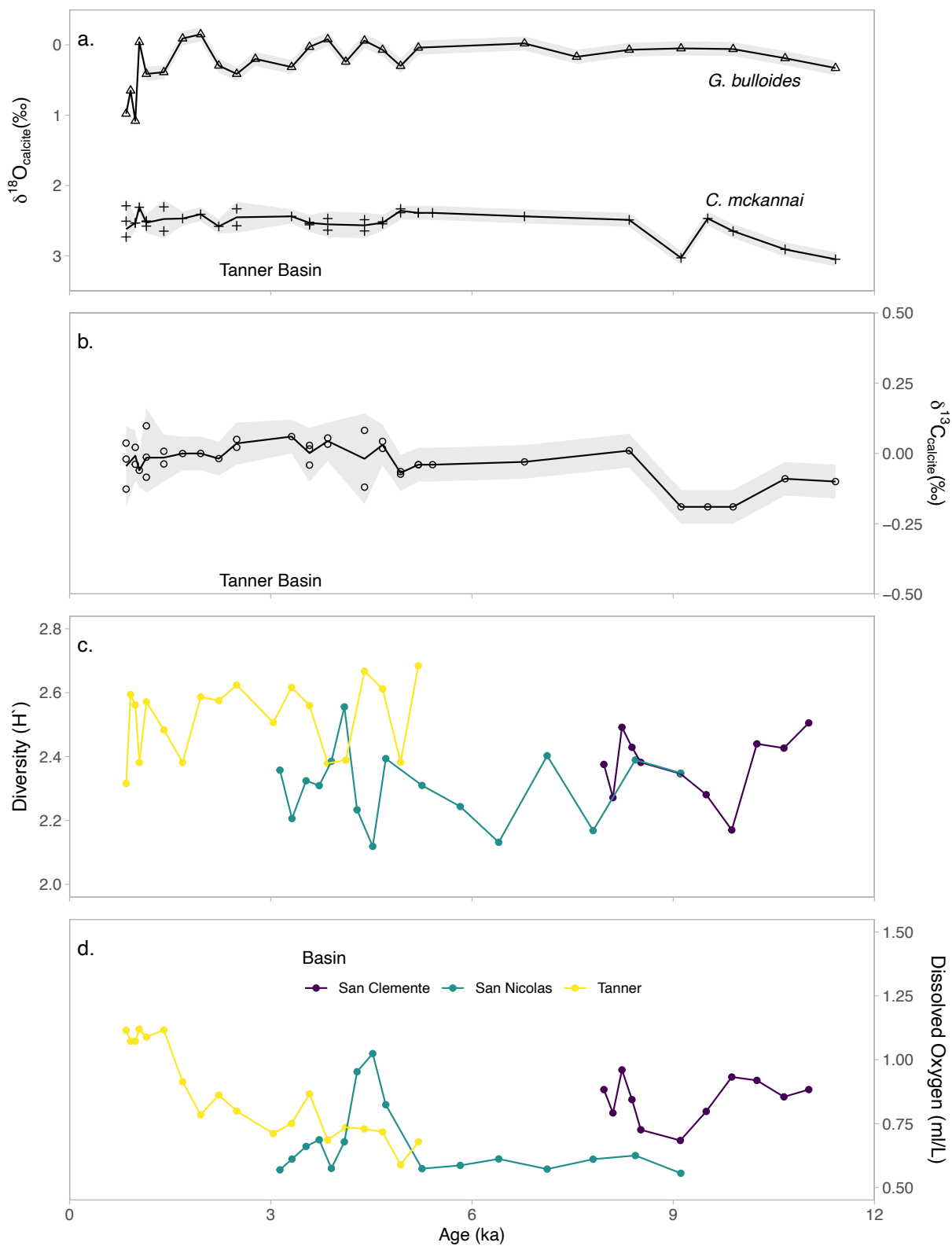
**3.6 Metazoan microfossil analysis**

447 Urchin spines and ostracods were present in the Tanner Basin core, but do not present a coeval trend;

448 urchins are present in 13 of 19 intervals, ostracods are present in 5 of 19 samples. Urchin spines and

449 ostracods were scarce in sediments from San Nicolas Basin: urchin spines are present in 6 of 17 and

450 ostracods are present in 2 of 17 intervals. Ostracods and urchin spines were nearly ubiquitous (present in

451 every interval except one) in San Clemente Basin (Figure S5).

452

**3.7 Modern oxygenation in the Southern California Borderlands**

454 Modern oxygenation decreases linearly with depth from 1000 to 2000 m in this region, and ranges from

455 0.15-1.67 ml $L^{-1}$ and has a mean of 0.78 ml $L^{-1}$ across all depths (1000-2000m). Modern oxygenation in

456 the 50 m above and below the Tanner Basin site (1144-1244 m) has a mean of 0.77 ± 0.18 ml $L^{-1}$. Modern

457 oxygenation in the 50 m above and below the San Nicolas Basin site (1392-1492 m) has a mean of 0.88 ±

458 0.37 ml $L^{-1}$. Modern oxygenation in the 50 m above and below the San Nicolas Basin site (1392-1492 m)

459 has a mean of 1.51 ± 0.09 ml $L^{-1}$.

| | Tanner Basin | | San Nicolas Basin | | San Clemente Basin | |
|---|---|---|---|---|---|---|
| | Mean | Range | Mean | Range | Mean | Range |
| Behl Index reconstructed oxygen (ml $L^{-1}$) | 0.86 | 0.59-1.12 | 0.67 | 0.56-1.02 | 0.84 | 0.68-0.96 |
| Schmiedl Index reconstructed oxygen (ml $L^{-1}$) | 1.73 | 1.59-1.81 | 1.50 | 1.36-1.66 | 1.60 | 1.48-1.71 |
| Modern dissolved oxygen (ml $L^{-1}$) | 0.77 | 0.31-1.45 | 0.88 | 0.28-1.39 | 1.51 | 1.39-1.61 |

460 **Table 1:** Reconstructed and modern dissolved oxygen values for Tanner, San Nicolas, and San Clemente

461 Basins. Modern oxygenation is from CalCOFI data from 50 m above and below the water depth of core

462 collection for each basin.

463

464

465

466    **Figure 3:** Stable isotope record from Tanner Basin (a., b.), benthic foraminiferal diversity (c.), and

467    reconstructed oxygenation (d.) for all three sites using Behl Dissolved Oxygen Index. Oxygen isotopes of

468    planktic foraminifera *G. bulloides* from this study and Stott et al., 2000 indicated as triangles (a.). Oxygen

469    and carbon isotopes of benthic foraminifera *C. mckannai* from this study and Stott et al., 2000 indicated

470    as + (b.). Analytical uncertainty for stable isotopes is shown as gray bar ($\delta^{13}$C ±0.06‰ and $\delta^{18}$O ±0.10‰).

471    In the isotope figures, data from 3.8-0.8 ka includes both data from Stott et al., 2000 and this study, data

472    from 11.4-3.8 ka is from Stott et al., 2000. For diversity and reconstructed dissolved oxygen yellow

473    indicates Tanner, green indicates San Nicolas, and purple indicated San Clemente). Oxygen is reported in

474    ml L$^{-1}$. **Discussion**

475    **4.1 Paleo-oxygenation reconstruction**

476    By analyzing the complete assemblage from each basin, we interpret a gradual shift in relative abundance

477    of taxa in Tanner Basin, multi-centennial shifts in the assemblage at San Nicolas Basin, and stability in

478    the assemblage in San Clemente Basin. Examining indicator taxa, we identify a decrease in suboxic taxon

479    *B. spissa* and a decrease in *U. peregrina* coeval with an increase in oxic indicator *Hansenisca* sp. in

480    Tanner Basin from 1.7 to 0.8 ka. In San Nicolas Basin, we observe a short period of divergence from the

481    mean assemblage driven by an increase in the oxic-associated taxon *C. mckannai* and a sharp decline in

482    *U. peregrina* from 4.7-4.3 ka. We observe little change over time in the relative abundance of these

483    indicator taxa in San Clemente Basin. We do not identify a relationship between NMDS and DCA species

484    scores and previously published categories of oxygenation indicating that oxygenation may not be the

485    dominant factor in determining the full assemblage. Other parameters such as proximity to the margin of

486    the OMZ, sediment grain size, and organic matter availability also play important roles in structuring

487    foraminiferal diversity and assemblage (e.g., Bernhard et al., 1997; Sharon et al., 2021; Venturelli et al.,

488    2018).

489

490    Reconstructed oxygen concentration differs between the two transfer functions compared here.

491    Reconstructed dissolved oxygen using Behl Index for all three cores yields values (0.56-1.12 ml L$^{-1}$)

492    within "intermediate hypoxia" as defined by Moffitt et al., and "suboxic" as defined by Cannariato and

493    Kennett and Kaiho (Cannariato & Kennett, 1999; Kaiho, 1994; Moffitt et al., 2014). Reconstructed values

494    using the Behl Index are similar to the range of modern values for bottom water oxygenation with notable

495    exceptions discussed below (Figure 3d, 4). In comparison, the Schmiedl Index output is higher (1.36-

496    1.81 ml L$^{-1}$) than the Behl Index by approximately 0.5 ml L$^{-1}$ (Figure S4). We posit that this is due to the

497    fact that diversity and oxygenation are not necessarily inversely correlated, particularly in intermediate

498    hypoxic environments, yet the Schmiedl Index is based on diversity. Oxygenation plays a more dominant

499    role in structuring diversity across biological thresholds (such as below 0.5 ml L-1 [$O_2$]) than across

500  oxygen gradients that do not cross biological thresholds (McGann, 2011; Palmer et al., 2020; Sharon et

501  al., 2021; Venturelli et al., 2018). Additionally, the Schmiedl index only considers the end member

502  groups: hypoxic and weakly suboxic/oxic, and does not include the relative abundance of suboxic taxa,

503  taxa which may be important community members and oxygenation indicators at this water depth. Thus,

504  we utilize the Behl Index to reconstruct absolute values of paleo-oxygenation (Figure 3).

505

506  **4.2 Ecological and environmental change through the Holocene in the Southern California**

507      **Borderlands**

508  Geochemical and faunal records from Tanner, San Nicolas, and San Clemente Basins indicate

509  environmental and ecological stability in water below 1000m through the Holocene in the Southern

510  California Borderlands. Planktic $\delta^{18}$O records from Tanner Basin indicate constant sea surface conditions

511  (salinity/temperature) through most of the Holocene (11.75 – 2.3 ka) and a decrease in sea surface

512  temperature or increase in salinity from 1.0-0.8 ka relative to the rest of the Holocene (Figure 3). Benthic

513  $\delta^{18}$O and $\delta^{13}$C of the epibenthic foraminifera *C. makannai* exhibit little change through the Holocene

514  (Figure 4). Reconstructed seafloor oxygenation using the Behl Index is within the range of intermediate

515  hypoxia (0.5 – 1.5 ml L$^{-1}$) and are similar to the range of modern values for bottom water oxygenation

516  with notable exceptions discussed below (Figure 3d, 4).

517

518  Ecological and environmental change over time as measured by diversity and multi-dimensional

519  community metrics also indicate stability through the Holocene. Diversity varied little between basins and

520  through time within each basin. Shannon Index of diversity (H) ranged from 2.12 to 2.68 across all sites

521  and points in time, and diversity did not significantly change through time at any site across this interval

522  (ANOVA, p>0.05) (Figure 3, S4). Results of NMDS and DCA show species assemblages are distinct in

523  each basin; at any time point, assemblages are more similar to other time points from the same basin than

524  to any other time point from an adjacent basin (Figure S2). This demonstrates that each basinal

525  environment is unique and the analysis of benthic foraminifera as environmental indicators must consider

526  local factors. We hypothesize that the stability in diversity and community-scale ecology indicates that

527  environmental conditions were also relatively stable through this interval. This evidence aligns with

528  results of oxygenation reconstruction from the Behl Index and stable isotope analysis (Figure 3).

529

530  Changes in benthic foraminifera morphology can reflect environmental variations that are missed by

531  community-based analyses. Comparison of two species (*U. peregrina*, *B. spissa*) between basins (studied

532  here) and open margin sediments (San Diego Margin, 300-1200 m water depth see Palmer et al., 2020)

533  shows that both species are larger in the nearshore environment relative to offshore basins (Tanner, San

534    Clemente Basin, see Figure S3). At this scale, we interpret the size difference to be representative of

535    higher relative organic matter input at coastal margin sites or warmer bottom water temperatures at

536    shallower coastal margin sites in comparison to offshore basins (Keating-Bitonti & Payne, 2016, 2018).

537    Importantly though, in comparison to changes between coastal margins and offshore basins, there is

538    relatively little change in shell size of *Quinqueloculina* sp. (oxic indicator species) or *B. spissa* (suboxic

539    indicator species) over time (5.4-0.8 ka) in Tanner Basin (Figure S3). Thus, benthic foraminiferal $\delta^{18}$O

540    and $\delta^{13}$C, reconstructed dissolved oxygen (Behl Index), community scale ecology, and morphology all

541    indicate relative stability in environmental conditions at water depths 1194-1818 m through the studied

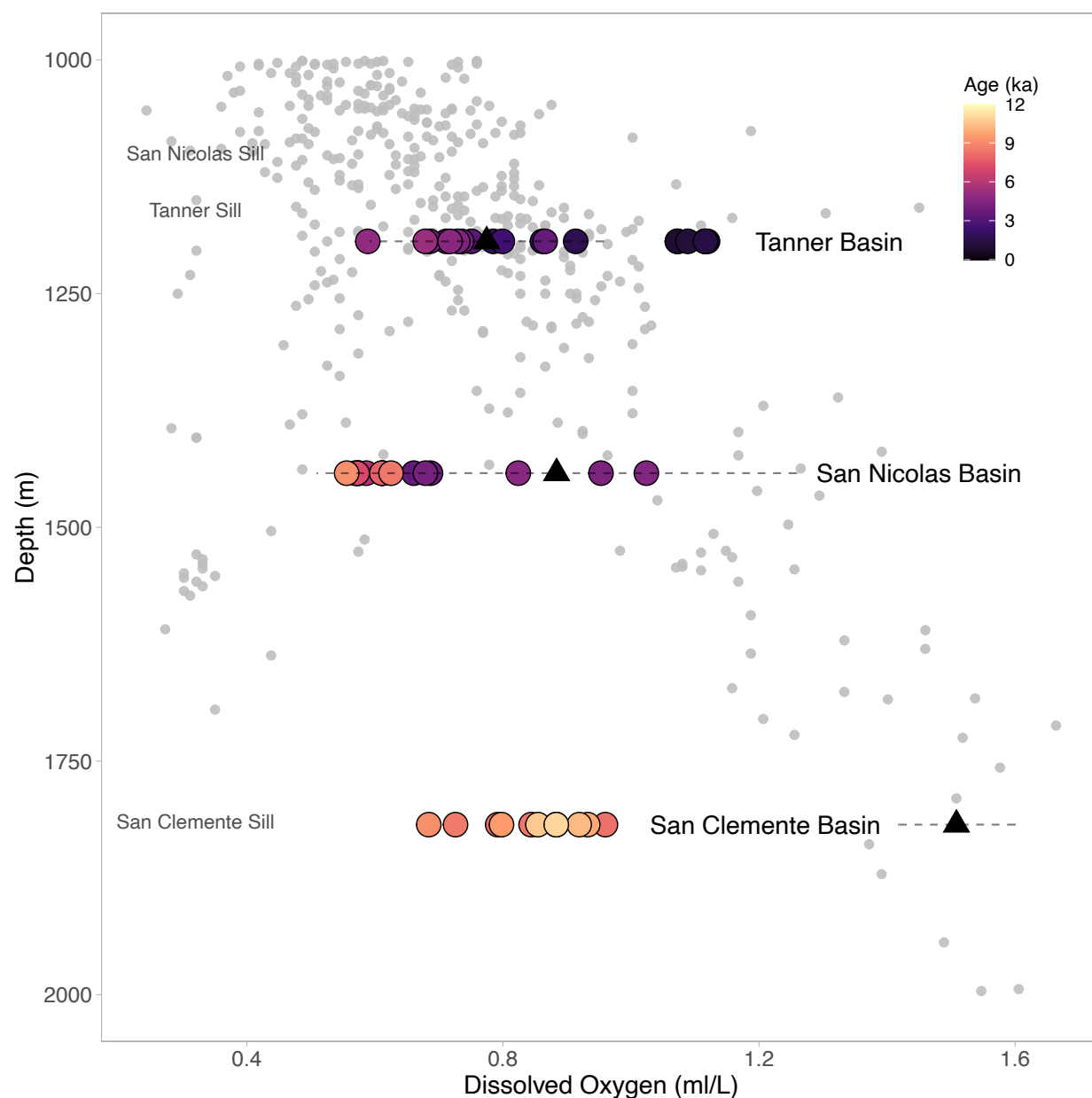542    time interval with few notable exceptions discussed below.

543

544    **4.2.1 Ecological and environmental change through time in Tanner Basin**

545    In Tanner Basin, the benthic foraminiferal assemblage shifts from more hypoxic taxa at 5.4-1.7 ka to

546    more oxic associated taxa from 1.7-0.8 ka (Figures 2, 3). This shift is largely driven by the increase in

547    *Hansenisca soldanii* (previously *Gyroidina soldanii*) and decrease in *B. spissa* and *U. peregrina* (Figure

548    2). *Hansenisca soldanii* has been documented in well oxygenated, oligotrophic, cold deep water with

549    pulsed food supply (De & Gupta, 2010), and both *B. spissa* and *U. peregrina* are well documented

550    indicators of low oxygen. Using the modified Behl Index, reconstructed oxygenation increases from 0.58

551    to 1.12 ml L$^{-1}$ across this interval (Figure 3). Thus, we interpret this assemblage shift as an indication of a

552    increase of approximately 0.4 ml L$^{-1}$ in Tanner Basin occurring around 1.7 ka.

553

554    Downcore morphometric analysis shows that neither relative abundance nor surface area of

555    *Quinqueloculina* sp. (an oxic indicator species) changes through time. Although *B. spissa* decreases in

556    relative abundance from 5.4-0.8 ka, shell size (surface area) does not change through time (Figure S3).

557    Stability in shell size concurrent with changes in relative abundance may indicate an interaction of factors

558    including oxygen and organic matter influx in determining lethal vs. sublethal effects on *B. spissa*.

559    Further, the lack of changes in shell size of *B. spissa* and *Quinqueloculina* across this interval may

560    indicate a consistent supply of surface-exported organic matter, the main food resource for these benthic

561    foraminifera. Ostracod and echinoderm presence are not correlated with increase in dissolved oxygen at

562    this site (Figure S5). We hypothesize that the shift identified in the benthic foraminiferal assemblage is in

563    response to a relatively small change in oxygenation (less than 1 ml L$^{-1}$) and does not represent

564    fluctuations across biologically important thresholds for metazoan taxa, as dissolved oxygen was never

565    below 0.4 ml L$^{-1}$ (Figure 3).

566

567    When compared to modern CalCOFI data, reconstructed oxygenation (using the Behl Index) is within $1\sigma$

568    of modern mean oxygenation (Figure 4), except for the interval from 1.7 – 0.8 ka in which reconstructed

569    oxygen is higher than modern by 0.3 ml $L^{-1}$ (Figure 4). There is no significant difference (ANOVA,

570    Tukey, p=0.51) between reconstructed oxygenation values (mean=0.86 ml $L^{-1}$) and all modern

571    oxygenation values (mean=0.77 ml $L^-1$) within waters 50 m above and below the Tanner Basin site

572    (Figure 4). Combining assemblage, oxygenation index, and isotopic records of Tanner Basin, we identify

573    increased dissolved oxygen in the basin from 1.7-0.8 ka relative to 5.4-1.7 ka that is not correlated with

574    changes in either the oxygen or carbon isotope records and remains within the modern range of dissolved

575    oxygen variability. The changes in Tanner Basin dissolved oxygen are minor when compared to changes

576    in oxygenation in nearby more shallow basins within the OMZ (Balestra et al., 2018; Moffitt et al., 2014;

577    Palmer et al., 2020; Wang et al., 2020).

578



579
580  **Figure 4:** Reconstructed dissolved oxygen concentration (ml L$^{-1}$) from Tanner, San Nicolas, and San

581  Clemente Basin (large dots colored by age) compared with modern dissolved oxygen concentration (ml L$^{-}$

582  $^1$) from CalCOFI bottle sampling (1986-2019) (shown in small gray dots). Depth of sill of each basin is

583  labeled. Black triangles show mean modern dissolved oxygen concentration from 50 m above and below

584  each site and dashed gray line shows 1σ range in modern dissolved oxygen concentration from 50 m

585  above and below each site.

586

587  **4.2.2 Ecological and environmental change through time in San Nicolas Basin**

588    In San Nicolas Basin, low oxygen-associated benthic foraminiferal taxa dominate from 9.8 to 4.7 ka. A

589    short period of anomalous assemblage driven by an increase in *C. mckannai,* an oxic-associated taxon,

590    and a sharp decline in *U. peregrina*, an intermediate hypoxia-associated taxon, occurs at 4.7-4.3 ka and is

591    interpreted as an interval of increased oxygenation. Using the modified Behl Index, reconstructed

592    oxygenation increases from 0.59 ml L$^{-1}$ before the interval to a maximum of 1.03 ml L$^{-1}$ during the

593    oxygenation interval (Figure 3). Oxygenation returned to pre-event levels of dissolved oxygen after 4.3 ka

594    and pre and post event assemblages are similar, indicating an absence of a legacy effect of the event on

595    the community (Figure 2). Metazoan invertebrate microfossils (ostracods and urchin spines) are scarce in

596    this core and changes in presence/absence of metazoans do not correlate with shifts in benthic

597    foraminiferal assemblages (Figure S5). Modern studies of circulation in San Nicolas Basin indicate that

598    residence time for bottom waters in the basin are $9 \pm 2$ months (Berelson, 1991). As such, we hypothesize

599    that the assemblage response recorded here represents persistent oxygenation or repeated ventilation on a

600    decadal-to-centennial scale, rather than a single episode of ventilation. Yet, the absolute change in

601    oxygenation is relatively minor and still within a threshold of intermediate hypoxia and within the range

602    of modern values (Figure 3, 4).

603

604    When compared to modern CalCOFI data, reconstructed oxygenation in San Nicolas Basin is slightly

605    lower than modern mean dissolved oxygen yet remains within 1σ of the modern mean at all points

606    throughout the Holocene (Figure 4). Reconstructed oxygenation (mean=0.67 ml L$^{-1}$) is statistically lower

607    than modern oxygenation from waters 50 m above and below the depth of the San Nicolas site (ANOVA,

608    Tukey $p<0.05$) (Figure 4). Further, the variance in reconstructed dissolved oxygen is similar to variance

609    in modern oxygenation at the sill depth of San Nicolas Basin (1100m, see Figure 4). The scale of change

610    in reconstructed dissolved oxygen, relative abundance of species, and species diversity in San Nicolas

611    Basin across this interval of change is minor when compared to intervals of change in nearby basins

612    across the deglacial and in comparison to Holocene changes within basins that experienced shifts between

613    anoxic and oxic conditions, such as the Macoma Event in the Santa Barbara Basin (Balestra et al., 2018;

614    Cannariato & Kennett, 1999; Moffitt et al., 2015; Praetorius et al., 2015; Schimmelmann et al., 2013).

615

616    **4.2.3 Ecological and environmental change through time in San Clemente Basin**

617    Environmental conditions remained relatively constant in San Clemente Basin from 11.0-8.0 ka as

618    demonstrated by the lack of variability in the benthic foraminiferal assemblages. Species diversity does

619    not change significantly through time (Figure 3, S4). Reconstructed oxygenation from the modified Behl

620    Index ranges from 0.67 to 0.96 ml L$^{-1}$ across this interval; this variability is reduced relative to Tanner and

621    San Nicolas Basins (Figure 3). The assemblage at this depth is distinct from coastal margin environments

622    and other, shallower basins (Balestra et al., 2018; Moffitt et al., 2014; Palmer et al., 2020). Ostracods and

623    urchin spines are present in every interval (except one) examined here, indicating a well-oxygenated

624    seafloor environment that supported metazoan life and motile organisms (Figure S5) (Moffitt et al.,

625    2015). Ecological differences between the shallow sill basins (San Nicolas and Tanner) vs. the deep sill

626    basin (San Clemente) documented here are mirrored in previously documented seafloor metazoan

627    assemblages (France, 1994). We hypothesize that at 1815 m water depth, this site was not impacted by

628    changes in the oxygen minimum zone during the Holocene and that intermediate and deep water reaching

629    this site had a consistent source from 11.0-8.0 ka.

630

631    In comparison to modern CalCOFI data, reconstructed dissolved oxygen (mean=0.84 ml $L^{-1}$) in the early

632    and mid-Holocene is statistically lower than modern dissolved oxygen (mean=1.50 ml $L^{-1}$) within 50 m

633    above and below the depth of the San Clemente Site ($p<0.05$) (Figure 4). We propose three potentially

634    overlapping hypotheses for this difference. First, this may be an artifact of categorizations of some

635    species used in the Behl Index that use lowest known thresholds of oxygenation and thus may predict the

636    minima of dissolved oxygen concentrations. Second, in the early Holocene, sea level was lower than

637    modern (by approximately 70 m), thus, the sites sampled here may have been less well oxygenated simply

638    due to being at a shallower depth, but this would not entirely explain the difference from modern (Figure

639    4) (Fleming et al., 1998; Moffitt et al., 2014). Finally, the preformed oxygenation of the incoming water

640    masses may have been lower than modern, a pattern that is reflected in Santa Monica and Santa Barbara

641    Basins at this time (Balestra et al., 2018; Wang et al., 2020).

642

643    **4.3 Environmental stability in Southern California Borderlands through the Holocene and**

644    **comparison to modern ocean conditions**

645    Environmental conditions in Tanner, San Nicolas, and San Clemente Basins remained relatively stable

646    across the time intervals examined. In the early to mid-Holocene (11.0-4.7 ka), seafloor oxygenation and

647    environmental conditions more broadly below 1400 m were stable in the Southern CA Borderlands,

648    evidenced by stability in assemblage records from San Clemente Basin (1815 m) and San Nicolas Basin

649    (1442 m), and was likely driven by consistent source and composition of intermediate waters. Benthic

650    foraminiferal assemblage records from the Santa Lucia Slope (ODP 1017, 955 m) offshore Point

651    Conception indicate a stable suboxic environment (reconstructed [$O_2$] 1.5-0.5 ml $L^{-1}$) through the early

652    and mid-Holocene and are similar in taxonomic composition to the records presented here from San

653    Nicolas and San Clemente Basins (Cannariato & Kennett, 1999; Sharon & Belanger, 2022). Synchrony in

654    stability and assemblages across San Nicolas Basin (1442 m), San Clemente Basin (1818 m), and the

655    Santa Lucia Slope (955 m) contrasts with evidence of fluctuations in age of North Pacific Intermediate

656     Water entering SBB (as recorded by benthic-planktic radiocarbon age differences) at 9 ka (Roark et al.,

657     2003), expansion of the OMZ in SBB in the early Holocene (Wang et al., 2020), and a turning point from

658     hypoxic to suboxic conditions at 9 ka in Santa Monica Basin (indicated by benthic foraminiferal

659     assemblages and geochemical records) (Balestra et al., 2018). Differences in oxygenation between sites

660     may be explained by differences across water depth; we propose that changes in the source and strength

661     of NPIW impacted sites at 400-1000m water depth (SBB, SMB) (Balestra et al., 2018; Roark et al., 2003;

662     Wang et al., 2020), but had less of an effect on the water column below 1000 m. Similar patterns of stable

663     suboxic conditions below the depth of the OMZ and variability in dissolved oxygen at shallower, OMZ-

664     impacted depths through the Holocene were observed further north, offshore British Columbia, and have

665     been attributed to changes in the strength of NPIW (Sharon & Belanger, 2022). In the mid to late

666     Holocene, San Nicolas Basin experienced a multi-centennial oxygenation interval from 4.7-4.3 ka and

667     oxygenation increased in Tanner Basin beginning at 1.0 ka, yet all changes were within 1 ml $L^{-1}$ [$O_2$] .

668     Drivers of oxygenation in each basin may have been due to "indirect" ventilation through diffusion of

669     dissolved oxygen from overlying waters, rather than "direct" ventilation due to advection (Talley, 1993),

670     a change in oxygenation of source waters, or basinal processes related to the shape, depth, and overlying

671     surface water productivity in each basin.

672

673     Although oxygenation does vary across the Holocene in Tanner, San Nicolas, and San Clemente basins,

674     all variability was within 1 ml $L^{-1}$ [$O_2$] and does not cross critical biological thresholds below 0.5 ml $L^{-1}$

675     or above 1.5 ml $L^{-1}$ in any basin. As such, variability in oxygenation and ventilation of San Nicolas,

676     Tanner, and San Clemente basins is reduced relative to shallower sites, including Santa Barbara Basin and

677     Santa Monica Basin, across the entire Holocene (Balestra et al., 2018; Moffitt et al., 2014; Ohkushi et al.,

678     2013). Additionally, Holocene-scale oxygenation changes (presented here) are reduced relative to

679     glacial/interglacial changes in oxygenation in the basins examined here and in the nearby Santa Lucia

680     Slope (Cannariato & Kennett, 1999; Stott et al., 2000). This indicates that Holocene-scale climate changes

681     driving oxygenation change shallower than 1000 m are not impacting waters below 1000 m and that

682     climate changes within the Holocene do not significantly impact oxygenation below 1000 m, despite

683     changes in the intensity and extent of the OMZ shallower than 1000 m. As such, we hypothesize that

684     deoxygenation due to anthropogenic climate change will also have a greater impact on the water column

685     above 1000 m, relative to below 1000m.

686

687     Direct comparison of reconstructed dissolved oxygen with modern measured dissolved oxygen indicates

688     that the variance across millennia is similar to decadal-scale variance in the modern ocean (Figure 4).

689     Variance in dissolved oxygen occurring on centennial to millennial timescales does not exceed the

690    variance observed in this modern ocean, indicating stability in intermediate waters and oxygenation below

691    1100 m in the Southern California Borderlands. We hypothesize that if there are significant changes to

692    oxygenation below 1000m due to anthropogenic climate change, these changes may have large impacts

693    on benthic ecosystems as they have not experienced significant changes in dissolved oxygen over the last

694    11 ka.

695

696    **5   Conclusion**

697    Reconstruction of past oxygenation using analysis of benthic microfaunal communities (foraminiferal and

698    metazoan) is optimized by combining multiple approaches including analysis of indicator taxa,

699    reconstruction of oxygenation using multi-taxa indices, and community scale-analysis such as

700    multidimensional analysis and diversity. Here we demonstrate the utility of combined approaches, and we

701    expand the use of the Behl Index for paleo-oxygenation reconstruction. Analysis of benthic foraminiferal

702    assemblages from three silled basins (Tanner, San Nicolas, San Clemente) in the Southern California

703    Borderlands combined with benthic and planktic stable isotope analysis from Tanner Basin show largely

704    stable oxygenation except for a gradual increase (approximately 0.4 ml $L^{-1}$ [$O_2$]) in oxygenation in Tanner

705    Basin occurring at 1.7 ka and multi-centennial variability in oxygenation (approximately 0.5 ml $L^{-1}$ [$O_2$])

706    in San Nicolas Basin. The seafloor environment is stable in San Clemente Basin from 11.0-8.0 ka, yet

707    reconstructed oxygenation is lower than modern at this site. Holocene scale climate changes did not drive

708    significant changes (> 1 ml $L^{-1}$) in marine oxygenation below 1000 m in the Southern California

709    Borderlands. In the context of modern oxygenation changes, findings from this analysis show that

710    seafloor oxygenation of the Southern California Borderlands through the Holocene below 1000 m

711    remained relatively stable and variance in oxygenation across millennia is similar to decadal-scale

712    variance in the modern ocean. As such, we expect that future changes to marine oxygenation will be

713    greater at depths above 1000 m relative to deeper waters and note that if anthropogenic climate change

714    induced changes in oxygenation do cause shifts in dissolved oxygen greater than > 1 ml $L^{-1}$ below 1000

715    m, it will represent a divergence from scales of variability over the last 11 ka.

716

725

726    **Open Research**

727    The benthic foraminiferal assemblage data, radiocarbon age model data, carbon and oxygen stable isotope

728    data, and morphometric data used for environmental reconstruction in the study are available at Dryad via

729    Palmer et al. (2022).

730

**References**

Addison, J. A., Barron, J., Finney, B., Kusler, J., Bukry, D., Heusser, L. E., & Alexander, C. R. (2017). A Holocene record of ocean productivity and upwelling from the northern California continental slope. *Quaternary International*.

Balestra, B., Krupinski, N. B. Q., Erohina, T., Fessenden-Rahn, J., Rahn, T., & Paytan, A. (2018). Bottom-water oxygenation and environmental change in Santa Monica Basin, Southern California during the last 23 kyr. *Palaeogeography, Palaeoclimatology, Palaeoecology*, *490*, 17–37.

Barron, J. A., Heusser, L., Herbert, T., & Lyle, M. (2003). High-resolution climatic evolution of coastal northern California during the past 16,000 years. *Paleoceanography*, *18*(1).

Behl, R. J., & Kennett, J. P. (1996). Brief interstadial events in the Santa Barbara basin, NE Pacific, during the past 60 kyr. *Nature*, *379*(6562), 243–246. https://doi.org/DOI 10.1038/379243a0

Belanger, C. L., Jablonski, D., Roy, K., Berke, S. K., Krug, A. Z., & Valentine, J. W. (2012). Global environmental predictors of benthic marine biogeographic structure. *Proceedings of the National Academy of Sciences*, *109*(35), 14046–14051. https://doi.org/10.1073/pnas.1212381109

Belanger, C. L., Sharon, Du, J., Payne, C. R., & Mix, A. C. (2020). North Pacific deep-sea ecosystem responses reflect post-glacial switch to pulsed export productivity, deoxygenation, and destratification. *Deep Sea Research Part I: Oceanographic Research Papers*, *164*, 103341. https://doi.org/10.1016/j.dsr.2020.103341

Berelson, W. M. (1991). The flushing of two deep-sea basins, southern California borderland. *Limnology and Oceanography*, *36*(6), 1150–1166. https://doi.org/10.4319/lo.1991.36.6.1150

Berelson, W. M., & Stott, L. D. (2003). Productivity and organic carbon rain to the California margin seafloor: Modern and paleoceanographic perspectives. *Paleoceanography*, *18*(1), 2-1-2–15. https://doi.org/10.1029/2001PA000672

Bernhard, J. M., & Gupta, B. K. S. (1999). Foraminifera of oxygen-depleted environments. In *Modern foraminifera* (pp. 201–216). Springer.

757    Bernhard, J. M., Sen Gupta, B. K., & Borne, P. F. (1997). Benthic foraminiferal proxy to estimate dysoxic

758            bottom-water oxygen concentrations; Santa Barbara Basin, US Pacific continental margin. *The*

759            *Journal of Foraminiferal Research*, *27*(4), 301–310.

760    Bernhard, J. M., Visscher, P. T., & Bowser, S. S. (2003). Submillimeter life positions of bacteria, protists,

761            and metazoans in laminated sediments of the Santa Barbara Basin. *Limnology and*

762            *Oceanography*, *48*(2), 813–828.

763    Bograd, S. J., Buil, M. P., Lorenzo, E. D., Castro, C. G., Schroeder, I. D., Goericke, R., Anderson, C. R.,

764            Benitez-Nelson, C., & Whitney, F. A. (2015). Changes in source waters to the Southern

765            California Bight. *Deep Sea Research Part II: Topical Studies in Oceanography*, *112*, 42–52.

766            https://doi.org/10.1016/j.dsr2.2014.04.009

767    Bograd, S. J., Castro, C. G., Di Lorenzo, E., Palacios, D. M., Bailey, H., Gilly, W., & Chavez, F. P.

768            (2008). Oxygen declines and the shoaling of the hypoxic boundary in the California Current.

769            *Geophysical Research Letters*, *35*(12). https://doi.org/Artn L12607 10.1029/2008gl034185

770    Bograd, S. J., Checkley, D. A., & Wooster, W. S. (2003). CalCOFI: A half century of physical, chemical,

771            and biological research in the California Current System. *Deep Sea Research Part II: Topical*

772            *Studies in Oceanography*, *50*(14), 2349–2353. https://doi.org/10.1016/S0967-0645(03)00122-X

773    Bograd, S. J., & Lynn, R. J. (2003). Long-term variability in the Southern California Current System.

774            *Deep Sea Research Part II: Topical Studies in Oceanography*, *50*(14), 2355–2370.

775            https://doi.org/10.1016/S0967-0645(03)00131-0

776    Bograd, S. J., Schroeder, I. D., & Jacox, M. G. (2019). A water mass history of the Southern California

777            current system. *Geophysical Research Letters*, *46*(12), 6690–6698.

778            https://doi.org/10.1029/2019GL082685

779    Breitburg, D., Levin, L. A., Oschlies, A., Gregoire, M., Chavez, F. P., Conley, D. J., Garcon, V., Gilbert,

780            D., Gutierrez, D., Isensee, K., Jacinto, G. S., Limburg, K. E., Montes, I., Naqvi, S. W. A., Pitcher,

781            G. C., Rabalais, N. N., Roman, M. R., Rose, K. A., Seibel, B. A., … Zhang, J. (2018). Declining

782    oxygen in the global ocean and coastal waters. *Science*, *359*(6371), 46-+.

783    https://doi.org/10.1126/science.aam7240

784    Cannariato, K. G., & Kennett, J. P. (1999). Climatically related millennial-scale fluctuations in strength of

785    California margin oxygen-minimum zone during the past 60 k.y. *Geology*, *27*(11), 975–978.

786    https://doi.org/Doi 10.1130/0091-7613(1999)027<0975:Crmsfi>2.3.Co;2

787    Cardich, J., Gutiérrez, D., Romero, D., Pérez, A., Quipúzcoa, L., Marquina, R., Yupanqui, W., Solís, J.,

788    Carhuapoma, W., Sifeddine, A., & Rathbun, A. (2015). Calcareous benthic foraminifera from

789    the upper central Peruvian margin: Control of the assemblage by pore water redox and

790    sedimentary organic matter. *Marine Ecology Progress Series*, *535*, 63–87.

791    https://doi.org/10.3354/meps11409

792    Cardich, J., Sifeddine, A., Salvatteci, R., Romero, D., Briceño-Zuluaga, F., Graco, M., Anculle, T.,

793    Almeida, C., & Gutiérrez, D. (2019). Multidecadal Changes in Marine Subsurface Oxygenation

794    Off Central Peru During the Last ca. 170 Years. *Frontiers in Marine Science*, *6*.

795    https://doi.org/10.3389/fmars.2019.00270

796    Caulle, C., Koho, K. A., Mojtahid, M., Reichart, G. J., & Jorissen, F. J. (2014). Live (Rose Bengal

797    stained) foraminiferal faunas from the northern Arabian Sea: Faunal succession within and below

798    the OMZ. *Biogeosciences*, *11*(4), 1155–1175. https://doi.org/10.5194/bg-11-1155-2014

799    Checkley, D. M., & Barth, J. A. (2009). Patterns and processes in the California Current System.

800    *Progress in Oceanography*, *83*(1–4), 49–64. https://doi.org/10.1016/j.pocean.2009.07.028

801    Christensen, C. J., Gorsline, D. S., Hammond, D. E., & Lund, S. P. (1994). Non-annual laminations and

802    expansion of anoxic basin-floor conditions in Santa Monica Basin, California Borderland, over

803    the past four centuries. *Marine Geology*, *116*(3–4), 399–418.

804    De, S., & Gupta, A. K. (2010). Deep-sea faunal provinces and their inferred environments in the Indian

805    Ocean based on distribution of Recent benthic foraminifera. *Palaeogeography,*

806    *Palaeoclimatology, Palaeoecology*, *291*(3), 429–442.

807    https://doi.org/10.1016/j.palaeo.2010.03.012

808    Erdem, Z., Schönfeld, J., Rathburn, A. E., Perez, M.-E., Cardich, J., & Glock, N. (2019). Bottom-water

809        deoxygenation at the Peruvian Margin during the last deglaciation recorded by benthic

810        foraminifera. *Biogeosciences Discussions*. https://orcid.org/0000-0002-5509-8733

811    Evans, N., Schroeder, I. D., Buil, M. P., Jacox, M. G., & Bograd, S. J. (2020). Drivers of Subsurface

812        Deoxygenation in the Southern California Current System. *Geophysical Research Letters*, *47*(21),

813        e2020GL089274. https://doi.org/10.1029/2020GL089274

814    Fenton, I. S., Baranowski, U., Boscolo-Galazzo, F., Cheales, H., Fox, L., King, D. J., Larkin, C., Latas,

815        M., Liebrand, D., Miller, C. G., Nilsson-Kerr, K., Piga, E., Pugh, H., Remmelzwaal, S., Roseby,

816        Z. A., Smith, Y. M., Stukins, S., Taylor, B., Woodhouse, A., … Purvis, A. (2018). Factors

817        affecting consistency and accuracy in identifying modern macroperforate planktonic foraminifera.

818        *Journal of Micropalaeontology*, *37*(2), 431–443. https://doi.org/10.5194/jm-37-431-2018

819    Fisler, J., & Hendy, I. L. (2008). California Current System response to late Holocene climate cooling in

820        southern California. *Geophysical Research Letters*, *35*(9). https://doi.org/Artn L09702

821        10.1029/2008gl033902

822    Fleming, K., Johnston, P., Zwartz, D., Yokoyama, Y., Lambeck, K., & Chappell, J. (1998). Refining the

823        eustatic sea-level curve since the Last Glacial Maximum using far- and intermediate-field sites.

824        *Earth and Planetary Science Letters*, *163*(1), 327–342. https://doi.org/10.1016/S0012-

825        821X(98)00198-8

826    Forcino, F. L., Leighton, L. R., Twerdy, P., & Cahill, J. F. (2015). Reexamining Sample Size

827        Requirements for Multivariate, Abundance-Based Community Research: When Resources are

828        Limited, the Research Does Not Have to Be. *PLOS ONE*, *10*(6), e0128379.

829        https://doi.org/10.1371/journal.pone.0128379

830    France, S. C. (1994). Genetic population structure and gene flow among deep-sea

831        amphipods,Abyssorchomene spp., from six California Continental Borderland basins. *Marine

832        Biology*, *118*(1), 67–77. https://doi.org/10.1007/BF00699220

833    Gardner, J. V., Heusser, L. E., Quinterno, P. J., Stone, S. M., Barron, J. A., & Poore, R. Z. (1988). Clear

834          Lake record vs. The adjacent marine record; A correlation of their past 20,000 years of

835          paleoclimatic and paleoceanographic responses. In *Geological Society of America Special Papers*

836          (Vol. 214, pp. 171–182). Geological Society of America. https://doi.org/10.1130/SPE214-p171

837    Haslett, J., & Parnell, A. (2008). A simple monotone process with application to radiocarbon-dated depth

838          chronologies. *Journal of the Royal Statistical Society: Series C (Applied Statistics)*, *57*(4), 399–

839          418. https://doi.org/10.1111/j.1467-9876.2008.00623.x

840    Heaton, T. J., Köhler, P., Butzin, M., Bard, E., Reimer, R. W., Austin, W. E. N., Ramsey, C. B., Grootes,

841          P. M., Hughen, K. A., Kromer, B., Reimer, P. J., Adkins, J., Burke, A., Cook, M. S., Olsen, J., &

842          Skinner, L. C. (2020). Marine20—The Marine Radiocarbon Age Calibration Curve (0–55,000 cal

843          BP). *Radiocarbon*, *62*(4), 779–820. https://doi.org/10.1017/RDC.2020.68

844    Helly, J. J., & Levin, L. A. (2004). Global distribution of naturally occurring marine hypoxia on

845          continental margins. *Deep-Sea Research Part I-Oceanographic Research Papers*, *51*(9), 1159–

846          1168. https://doi.org/10.1016/j.dsr.2004.03.009

847    Ingram, B. L., & Southon, J. R. (1996). Reservoir ages in eastern Pacific coastal and estuarine waters.

848          *Radiocarbon*, *38*(3), 573–582.

849    Jaccard, S. L., Galbraith, E. D., Frolicher, T. L., & Gruber, N. (2014). Ocean (De)Oxygenation across the

850          Last Deglaciation Insights for the Future. *Oceanography*, *27*(1), 26–35.

851    Kaiho, K. (1994). Benthic Foraminiferal Dissolved-Oxygen Index and Dissolved-Oxygen Levels in the

852          Modern Ocean. *Geology*, *22*(8), 719–722. https://doi.org/Doi 10.1130/0091-

853          7613(1994)022<0719:Bfdoia>2.3.Co;2

854    Kaiho, K. (1999). Effect of organic carbon flux and dissolved oxygen on the benthic foraminiferal oxygen

855          index (BFOI). *Marine Micropaleontology*, *37*(1), 67–76. https://doi.org/Doi 10.1016/S0377-

856          8398(99)00008-0

857    Keating-Bitonti, C. R., & Payne, J. L. (2016). Physicochemical controls on biogeographic variation of

858          benthic foraminiferal test size and shape. *Paleobiology*, *42*(4), 595–611.

859    Keating-Bitonti, C. R., & Payne, J. L. (2017). Ecophenotypic responses of benthic foraminifera to oxygen

860        availability along an oxygen gradient in the California Borderland. *Marine Ecology*, *38*(3).

861    Keating-Bitonti, C. R., & Payne, J. L. (2018). Environmental influence on growth history in marine

862        benthic foraminifera. *Paleobiology*, *44*(4), 736–757. https://doi.org/10.1017/pab.2018.19

863    Kemp, A. C., Wright, A. J., & Cahill, N. (2020). Enough is Enough, or More is More? Testing the

864        Influence of Foraminiferal Count Size on Reconstructions of Paleo-Marsh Elevation. *Journal of*

865        *Foraminiferal Research*, *50*(3), 266–278. https://doi.org/10.2113/gsjfr.50.3.266

866    Levin, L. A., Ekau, W., Gooday, A. J., Jorissen, F., Middelburg, J. J., Naqvi, S. W. A., Neira, C.,

867        Rabalais, N. N., & Zhang, J. (2009). Effects of natural and human-induced hypoxia on coastal

868        benthos. *Biogeosciences*, *6*(10), 2063–2098. https://doi.org/10.5194/bg-6-2063-2009

869    McGann, M. (2011). Paleoceanographic changes on the Farallon Escarpment off central California during

870        the last 16,000 years. *Quaternary International*, *235*, 26–39.

871        https://doi.org/10.1016/j.quaint.2010.09.005

872    Moffitt, S. E., Hill, T. M., Ohkushi, K., Kennett, J. P., & Behl, R. J. (2014). Vertical oxygen minimum

873        zone oscillations since 20 ka in Santa Barbara Basin: A benthic foraminiferal community

874        perspective. *Paleoceanography*, *29*(1), 44–57. https://doi.org/10.1002/2013pa002483

875    Moffitt, S. E., Hill, T. M., Roopnarine, P. D., & Kennett, J. P. (2015). Response of seafloor ecosystems to

876        abrupt global climate change. *Proceedings of the National Academy of Sciences of the United*

877        *States of America*, *112*(15), 4684–4689. https://doi.org/10.1073/pnas.1417130112

878    Murgese, D. S., & De Deckker, P. (2005). The distribution of deep-sea benthic foraminifera in core tops

879        from the eastern Indian Ocean. *Marine Micropaleontology*, *56*(1), 25–49.

880        https://doi.org/10.1016/j.marmicro.2005.03.005

881    Myhre, S. E., Kroeker, K. J., Hill, T. M., Roopnarine, P., & Kennett, J. P. (2017). Community benthic

882        paleoecology from high-resolution climate records: Mollusca and foraminifera in post-glacial

883        environments of the California margin. *Quaternary Science Reviews*, *155*, 179–197.

884        https://doi.org/10.1016/j.quascirev.2016.11.009

885  Ohkushi, K., Kennett, J. P., Zeleski, C. M., Moffitt, S. E., Hill, T. M., Robert, C., Beaufort, L., & Behl, R.

886      J. (2013). Quantified intermediate water oxygenation history of the NE Pacific: A new benthic

887      foraminiferal record from Santa Barbara basin. *Paleoceanography*, *28*(3), 453–467.

888      https://doi.org/10.1002/palo.20043

889  Oksanen, J., Blanchet, F. G., Kindt, R., Legendre, P., Minchin, P. R., O'hara, R. B., Simpson, G. L.,

890      Solymos, P., Stevens, M. H. H., & Wagner, H. (2013). Package 'vegan.' *Community Ecology*

891      *Package, Version*, *2*(9).

892  Oschlies, A., Brandt, P., Stramma, L., & Schmidtko, S. (2018). Drivers and mechanisms of ocean

893      deoxygenation. *Nature Geoscience*, *11*(7), 467–473. https://doi.org/10.1038/s41561-018-0152-2

894  Palmer, H. M., Hill, T., Kennedy, E., Roopnarine, P., Langlois, S., Reyes, K., & Stott, L. (2022). *Data*

895      *from: Ecological and environmental stability in offshore Southern California Marine Basins*

896      *through the Holocene* (Version 6, p. 121877 bytes) [Data set]. Dryad.

897      https://doi.org/10.6071/M3Q090

898  Palmer, H. M., Hill, T. M., Roopnarine, P. D., Myhre, S. E., Reyes, K. R., & Donnenfield, J. T. (2020).

899      Southern California margin benthic foraminiferal assemblages record recent centennial-scale

900      changes in oxygen minimum zone. *Biogeosciences*, *17*(11), 2923–2937.

901      https://doi.org/10.5194/bg-17-2923-2020

902  Praetorius, S. K., Mix, A. C., Walczak, M. H., Wolhowe, M. D., Addison, J. A., & Prahl, F. G. (2015).

903      North Pacific deglacial hypoxic events linked to abrupt ocean warming. *Nature*, *527*(7578), 362-

904      +. https://doi.org/10.1038/nature15753

905  R Core Team. (2021). *R: A language and environment for statistical computing. R Foundation for*

906      *Statistical Computing*. https://www.R-project.org/

907  Rathburn, A. E., Willingham, J., Ziebis, W., Burkett, A. M., & Corliss, B. H. (2018). A New biological

908      proxy for deep-sea paleo-oxygen: Pores of epifaunal benthic foraminifera. *Scientific Reports*,

909      *8*(1), 9456. https://doi.org/10.1038/s41598-018-27793-4

910   Roark, E. B., Ingram, B. L., Southon, J., & Kennett, J. P. (2003). Holocene foraminiferal radiocarbon

911         record of paleocirculation in the Santa Barbara Basin. *Geology*, *31*(4), 379–382.

912         https://doi.org/Doi 10.1130/0091-7613(2003)031<0379:Hfrrop>2.0.Co;2

913   Schimmelmann, A., Hendy, I. L., Dunn, L., Pak, D. K., & Lange, C. B. (2013). Revised similar to 2000-

914         year chronostratigraphy of partially varved marine sediment in Santa Barbara Basin, California.

915         *Gff*, *135*(3–4), 258–264. https://doi.org/10.1080/11035897.2013.773066

916   Schmidtko, S., Stramma, L., & Visbeck, M. (2017). Decline in global oceanic oxygen content during the

917         past five decades. *Nature*, *542*(7641), 335-+. https://doi.org/10.1038/nature21399

918   Schmiedl, G., Mitschele, A., Beck, S., Emeis, K.-C., Hemleben, C., Schulz, H., Sperling, M., & Weldeab,

919         S. (2003). Benthic foraminiferal record of ecosystem variability in the eastern Mediterranean Sea

920         during times of sapropel S5 and S6 deposition. *Palaeogeography, Palaeoclimatology,*

921         *Palaeoecology*, *190*, 139–164. https://doi.org/10.1016/S0031-0182(02)00603-X

922   Schmiedl, G., Pfeilsticker, M., Hemleben, C., & Mackensen, A. (2004). Environmental and biological

923         effects on the stable isotope composition of recent deep-sea benthic foraminifera from the

924         western Mediterranean Sea. *Marine Micropaleontology*, *51*(1–2), 129–152.

925   Sharon, Belanger, C., Du, J., & Mix, A. (2021). Reconstructing Paleo-oxygenation for the Last 54,000

926         Years in the Gulf of Alaska Using Cross-validated Benthic Foraminiferal and Geochemical

927         Records. *Paleoceanography and Paleoclimatology*, *36*(2), e2020PA003986.

928         https://doi.org/10.1029/2020PA003986

929   Sharon, & Belanger, C. L. (2022). Placing North Pacific paleo-oxygenation records on a common scale

930         using multivariate analysis of benthic foraminiferal assemblages. *Quaternary Science Reviews*,

931         *280*, 107412. https://doi.org/10.1016/j.quascirev.2022.107412

932   Stott, L. D., Neumann, M., & Hammond, D. (2000). Intermediate water ventilation on the northeastern

933         Pacific margin during the late Pleistocene inferred from benthic foraminiferal delta C-13.

934         *Paleoceanography*, *15*(2), 161–169. https://doi.org/Doi 10.1029/1999pa000375

935    Stramma, L., Johnson, G. C., Firing, E., & Schmidtko, S. (2010). Eastern Pacific oxygen minimum zones:

936        Supply paths and multidecadal changes. *Journal of Geophysical Research: Oceans*, *115*(C9).

937    Stramma, L., Schmidtko, S., Levin, L. A., & Johnson, G. C. (2010). Ocean oxygen minima expansions

938        and their biological impacts. *Deep-Sea Research Part I-Oceanographic Research Papers*, *57*(4),

939        587–595. https://doi.org/10.1016/j.dsr.2010.01.005

940    Stuiver, M., & Polach, H. A. (1977). Discussion reporting of 14 C data. *Radiocarbon*, *19*(3), 355–363.

941    Talley, L. D. (1993). Distribution and Formation of North Pacific Intermediate Water. *Journal of Physical

942        Oceanography*, *23*(3), 517–537. https://doi.org/10.1175/1520-

943        0485(1993)023<0517:DAFONP>2.0.CO;2

944    Taylor, M. A., Hendy, I. L., & Pak, D. K. (2015). The California Current System as a transmitter of

945        millennial scale climate change on the northeastern Pacific margin from 10 to 50 ka.

946        *Paleoceanography*, *30*(9), 1168–1182. https://doi.org/10.1002/2014pa002738

947    Tetard, M., Licari, L., Tachikawa, K., Ovsepyan, E., & Beaufort, L. (2021). Toward a global calibration

948        for quantifying past oxygenation in oxygen minimum zones using benthic Foraminifera.

949        *Biogeosciences Discussions*, 1–17. https://doi.org/10.5194/bg-2020-482

950    Venturelli, R. A., Rathburn, A., Burkett, A., & Ziebis, W. (2018). Epifaunal Foraminifera in an Infaunal

951        World: Insights Into the Influence of Heterogeneity on the Benthic Ecology of Oxygen-Poor,

952        Deep-Sea Habitats. *Frontiers in Marine Science*, *5*, 344.

953    Wang, Y., Hendy, I. L., & Zhu, J. (2020). Expansion of the Southern California oxygen minimum zone

954        during the early-to mid-Holocene due to reduced ventilation of the Northeast Pacific. *Quaternary

955        Science Reviews*, *238*, 106326. https://doi.org/10.1016/j.quascirev.2020.106326

956